



Published in final edited form as:

Arch Gen Psychiatry. 2009 September ; 66(9): 938–946. doi:10.1001/archgenpsychiatry.2009.115.

Differential Targeting of the CA1 Subfield of the Hippocampal Formation by Schizophrenia and Related Psychotic Disorders

Scott A. Schobel, MD², Nicole M. Lewandowski, PhD¹, Cheryl M. Corcoran, MD², Holly Moore, PhD², Truman Brown, PhD³, Dolores Malaspina, MD, MSPH⁴, and Scott A. Small, MD¹

¹ Department of Neurology, Columbia University, College of Physicians and Surgeons, New York, New York

² Department of Psychiatry, Columbia University, College of Physicians and Surgeons, New York, New York

³ Department of Radiology, Columbia University, College of Physicians and Surgeons, New York, New York

⁴ Department of Psychiatry, New York University Medical Center, New York, New York

Abstract

Context—Because schizophrenia and related disorders have a chronic time course and subtle histopathology, it is difficult to identify which brain regions are differentially targeted.

Objective—To identify brain sites differentially targeted by schizophrenia, we applied a high-resolution variant of functional magnetic resonance imaging to clinically characterized patients and matched healthy controls and to a cohort of prodromal subjects who were prospectively followed up. Additionally, to explore the potential confound of medication use, the fMRI variant was applied to rodents receiving an antipsychotic agent.

Design—Cross-sectional and prospective cohort designs.

Setting—Hospital clinic and magnetic resonance imaging laboratory.

Participants—Eighteen patients with schizophrenia, 18 controls comparable in age and sex, and 18 prodromal patients followed up prospectively for 2 years. Ten C57-B mice received an antipsychotic agent or vehicle control.

Main Outcome Measures—Regional cerebral blood volume (CBV), as measured with magnetic resonance imaging, and symptom severity, as measured with clinical rating scales.

Results—In a first between-group analysis that compared patients with schizophrenia with controls, results revealed abnormal CBV increases in the CA1 subfield and the orbitofrontal cortex and abnormal CBV decreases in the dorsolateral prefrontal cortex. In a second longitudinal analysis, baseline CBV abnormalities in the CA1 subfield differentially predicted clinical progression to psychosis from a prodromal state. In a third correlational analysis, CBV levels in the CA1 subfield differentially correlated with clinical symptoms of psychosis. Finally, additional analyses of the human data set and imaging studies in mice suggested that antipsychotic agents were not confounding the primary findings.

Correspondence: Scott A. Small, MD, 630 W 168th St, New York, NY 10032 (sas68@columbia.edu).

Financial Disclosure: None reported.

Additional Contributions: We thank Ana Pereira, MD, and David Kimhy, PhD, for their aid in acquiring and analyzing data and Ella Campi, JD, for her helpful comments on the completed manuscript.

Conclusions—Taken as a whole, the results suggest that the CA1 subfield of the hippocampal subregion is differentially targeted by schizophrenia and related psychotic disorders. Interpreted in the context of previous studies, these findings inform underlying mechanisms of illness progression.

The frontal cortex, basal ganglia, amygdala, and hippocampal formation—all brain areas implicated in schizophrenia¹—are subdivided into functionally distinct subregions (Figure 1). Each subregion is unique in its molecular expression profile² so that select regions are differentially vulnerable to mechanisms of disease.³ Nevertheless, pinpointing regions differentially targeted by schizophrenia is difficult. By the time patients are clinically diagnosed with schizophrenia, multiple brain sites are affected,⁴ making the task of dissociating primary from secondary sites of dysfunction challenging. Further confounding the problem is the absence of pathognomonic histological markers or florid neurodegeneration.⁴ Thus, because schizophrenia is primarily a disease of neuronal dysfunction, not neuronal cell death, cross-sectional comparisons of postmortem samples do not necessarily reveal patterns of anatomical progression.

Two recent developments can be exploited to overcome these challenges. First, clinical criteria have been established that identify a high-risk prodromal group that, although clinically heterogeneous, is enriched with subjects in the earliest stages of the disease.^{5–7} Approximately 35% of prodromal patients progress clinically within a few years⁸; therefore, a relatively short prospective study can provide a snapshot of brain regions differentially targeted during early stages of the disease.

Second, variants of functional magnetic resonance imaging are now available that possess sufficient anatomic resolution to detect dysfunction in small subregions of the brain, including the hippocampal formation, the amygdala, and other implicated areas. Functional imaging relies on correlates of energy metabolism through either glucose uptake as an indicator of glucose metabolism or cerebral blood flow, cerebral blood volume, or deoxyhemoglobin as indicators of oxygen metabolism.^{9–12} Although an external sensory or cognitive stimulant can induce a transient change in brain metabolism, the internal stimulus of a disease state typically affects basal metabolic rates. There are many advantages to imaging disease-associated abnormalities in the basal state,¹³ in particular, the ability to slow image acquisition time, thereby significantly enhancing spatial resolution. As previously reviewed,¹⁴ the use of the contrast agent gadolinium to map basal cerebral blood volume (CBV) with magnetic resonance imaging is a functional imaging approach that provides high spatial resolution. Previous studies have shown that disease-associated basal defects in glucose uptake, as measured with positron emission tomography, tightly correlate with basal defects in CBV, as measured with magnetic resonance imaging.¹⁵ Intravenous injections of gadolinium can generate CBV maps using either a dynamic contrast enhancement approach or the steady state approach.¹⁴ For our purposes, the steady state approach is superior because it generates CBV with higher spatial resolution and because it relies on T1-weighted rather than T2*-weighted images. Both features are advantageous for imaging small subregions in the medial temporal lobe and the orbitofrontal cortex. In previous studies we have successfully used this approach to pinpoint dysfunction to individual hippocampal subregions in humans¹⁶ and non-human primates.¹⁷ Additionally, CBV mapping can be now used to generate high-resolution maps of the rodent hippocampal formation^{18,19} so questions that emerge from human studies can be explored in mouse models of disease.

To identify brain regions differentially targeted in schizophrenia, we completed 4 studies using high-resolution basal CBV mapping. First, because this imaging approach has not yet been applied to the disease, we compared patients with schizophrenia with matched controls. Second, using the findings from the first study as a guide, we tested which brain subregions predicted progression to psychosis from an ultra-high-risk state. Third, we performed

regression analyses that tested the association of CBV with clinical symptoms of psychosis. Fourth, to address the potential medication use confound, we performed additional analyses in human subjects and generated longitudinal CBV maps in mice exposed to an antipsychotic agent. Taken together, the results suggest a hippocampal subregion differentially targeted by schizophrenia and related disorders.

METHODS

HUMAN IMAGING

Subject Groups—We studied a total of 54 subjects (Table 1). The schizophrenia group met *DSM-IV* criteria for schizophrenia (n=14) or schizoaffective disorder (n=4) and were recruited from the inpatient and outpatient Lieber schizophrenia research clinics at the New York State Psychiatric Institute. The control group comprised healthy subjects comparable in age and sex with the patient group and were recruited within Columbia University Medical Center. The prodromal group was recruited from the Center of Prevention and Evaluation Clinic and met ultra-high-risk criteria for psychosis.⁵ All ultra-high-risk subjects were followed up longitudinally from the time of clinic enrollment and were typically evaluated every 3 months up to 2 years; none were lost to follow-up.

Clinical Assessment—Subjects in the schizophrenia and prodromal groups older than 18 years received the Diagnostic Interview for Genetic Studies²⁰ to confirm diagnosis, while subjects in the prodromal group received the Structured Interview for Prodromal Symptoms for clinic inclusion²¹ as well as the Kiddie Schedule for Affective Disorders and Schizophrenia interview if subjects were aged between 12 and 18 years.²² Symptom severity in the schizophrenia group was evaluated with the Positive and Negative Symptom Scale (PANSS) positive and negative symptom items²³ and with the Scale of Prodromal Symptoms (SOPS) in the prodromal group.²¹

CBV Mapping—As previously described,^{14,16,24} CBV maps were generated with a 1.5-T Philips Intera scanner (Andover, Massachusetts) using gadolinium pentate (Omniscan, 0.1mmol/kg; GE Healthcare, Chalfont St Giles, England). Briefly, a set of oblique coronal, 3-dimensional, T1-weighted, high-resolution (0.86×0.86 mm pixel size) images were acquired perpendicular to the hippocampal long axis before and 4 minutes after intravenous administration of the contrast agent. Subtracted images were then divided by the contrast-induced difference in signal measured from the superior sagittal sinus. Investigators blind to subject grouping (N.M.L. and S.A.S.) performed all image processing. The imaging protocol was approved through the Columbia University institutional review board.

Identifying Regions of Interest—Because of coregistration challenges when evaluating small brain regions in clinical populations, whole-brain voxel-based analyses are problematic; instead, we used a region-of-interest approach that relies on strict anatomical criteria to identify regions in areas previously implicated in schizophrenia (Figure 1).

Hippocampal Subregions: As previously described,¹⁶ by identifying the external morphology and internal architecture of the hippocampal formation, we can reliably parse the hippocampal subregions. As shown in Figure 1, this slice is invariably anterior in the hippocampal long axis, so we also demarcated a region of interest in a slice taken from the posterior hippocampus. In posterior slices, however, the entorhinal cortex no longer exists, and there is typically insufficient anatomical information to parse the individual hippocampal subregions.

Basal Ganglia: The ventral striatum CBV measurements were completed in a coronal section where the septum was best visualized. The anterior ventral portion of the head of the caudate, nucleus accumbens, and putamen were analyzed.

Frontal Lobes: The gyrus rectus, medial orbitofrontal gyrus, and dorsolateral prefrontal cortex were completed in the slice in which all 3 regions were best visualized. The dorsolateral prefrontal cortex was defined according to the criteria of Rajkowska and Goldman-Rakic.²⁵ Within this same slice, the gyrus rectus was identified and the medial orbital gyrus was selected as the gyrus immediately lateral to the gyrus rectus. Of note, signal artifact from braces excluded 1 prodromal subject from this analysis.

Amygdala: The dorsal and basolateral nuclei of the amygdala were measured according to the atlas by Mai and colleagues²⁶ as well as according to the methodology of Etkin et al.²⁷

MOUSE IMAGING

Generation of longitudinal CBV mapping in mice has been previously described (Figure 2).^{16,18} After a baseline image, C57/B6 mice were given 2 doses daily of risperidone (0.75 mg/kg/dose or 1.5 mg/kg/d) or its tartrate vehicle via oral gavage, and then reimaged following 3 weeks of treatment. Dosage was determined by previous binding and behavioral studies.^{28,29} All experiments were approved by and conducted according to the guidelines of the Institutional Animal Care and Use Committees of Columbia University Medical Center and The New York State Psychiatric Institute.

STATISTICAL ANALYSIS

The statistical models used for data analysis will be described according to the 4 studies. All statistical tests were 2-sided, and $\alpha=.05$.

Identifying Brain Regions Differentially Affected in Schizophrenia—A multivariate analysis of variance (ANOVA) model was constructed in which CBV values measured from the brain subregions were included as the dependent variables, diagnosis (schizophrenia vs controls) was included as the fixed factor, and demographics (age and sex) were included as covariates.

Identifying Brain Regions That Differentially Predict Clinical Progression of Prodromal Subjects—A multivariate ANOVA model was constructed in which CBV values identified in the first study were included as dependent variables, outcome (psychosis vs nonpsychosis) was included as the fixed factor, and demographics (age and sex) were included as covariates. Based on results of the first analysis, we dichotomized CA1 subfield metabolism at the overall mean value of the data set into high-CBV and low-CBV groups and constructed a 2×2 analysis with CA1 CBV as the categorical exposure variable and outcome to psychosis as the categorical disease variable. We then applied the Fischer exact test to the resultant 2×2 table.

Identifying Brain Regions Differentially Linked to Clinical Symptoms—The statistical reliability of any correlational analysis is strengthened by using a large number of subjects and by minimizing type I error incurred by multiple comparisons. Sensitive to these issues, we tried when possible to collapse symptom measures accumulated across schizophrenia and prodromal subjects. However, because of concerns that the 2 clinical constructs are not necessarily on a continuum, secondary analyses were performed for each group individually.

Positive Symptoms: Because the 5 positive items in the SOPS were directly developed from the PANSS,²¹ it was justifiable to collapse positive symptoms across subjects. Though the dynamic range of each scale is weighted differently, one toward a prepsychotic stage (SOPS) and the other toward frank psychosis (PANSS), the 2 scales test identical items. Thus, the 2 scales were unified into a single scale of positive symptom for each of those 5 psychotic items: PANSS 1=SOPS 0; PANSS 2=SOPS 3; PANSS 3=SOPS 4; PANSS 4 or 5=SOPS 6; PANSS 6 or 7=SOPS 7. For each of the positive items, PANSS ratings at the PANSS 3, or mild level, include the ability to reality-test or organize thought and are thus considered to be of prepsychotic severity. With progression to PANSS 4, or moderate level, this flexibility of thought form and content is lost and is thus equivalent to the SOPS 6 cutoff for psychosis. Finally, the PANSS contains levels of severe or extreme psychosis not reflected in the SOPS. Thus, the additional 7 designation was created to include PANSS items rated at a level of 6 or 7. The 5 items were added together to derive a total positive symptom summary score. All rating scale mean values by group are shown in Table 1.

A single linear regression model was constructed in which the total positive symptom score and the CBV values measured from regions identified in the first analysis were included as predictor variables and demographics were included as covariates.

Negative Symptoms: Because the negative symptom measurements in the PANSS and the SOPS are different, we could not generate a unified total negative symptom summary score between subject groups. Therefore, the linear regression analysis was performed individually for each summary score. A single linear regression model was constructed in which the total negative symptom score from each subscale (SOPS or PANSS) was the dependent variable and the CBV values measured from regions identified in the first analysis (CA1, orbitofrontal cortex, and dorsolateral prefrontal cortex) were included as predictor variables, and demographics were included as covariates.

Investigating the Potential Medication Use Confound—In addition to *t* tests between subjects treated with antidepressants or antipsychotics vs not, a categorical data analysis was also conducted to test whether antidepressant or antipsychotic exposure was associated with conversion status to psychosis and the Fischer exact test was applied. For the rodent treatment study, a repeated-measures ANOVA model was constructed in which CBV values from the hippocampal subregions before and after treatment were included as dependent variables and treatment (risperidone vs vehicle) was included as the fixed factor.

RESULTS

DISEASE-ASSOCIATED DYSFUNCTION DIFFERENTIALLY OBSERVED IN THE CA1 SUBFIELD, ORBITOFRONTAL CORTEX, AND DORSOLATERAL CORTEX

The multivariate component of the ANOVA model comparing the schizophrenia group with the control subjects revealed a significant group effect ($F = 3.8$; $P = .004$), and univariate components of the model revealed that this group effect was selectively driven by CBV increases in the schizophrenia group in the CA1 subfield ($F_{1,34} = 14.7$; $P = .001$) and orbitofrontal cortex ($F_{1,34} = 10.3$; $P = .003$) and CBV decreases in the dorsolateral cortex ($F_{1,34} = 4.5$; $P = .04$) (Figure 1B; Table 2). A trend was observed for the subiculum ($F_{1,34} = 3.5$; $P = .07$). Of note, mean areas of the regions of interest taken for CBV measurements did not differ across subjects in any brain subregion.

DIFFERENTIAL CA1 DYSFUNCTION OBSERVED IN EARLY STAGES OF DISEASE

After an average of 2 years of follow-up, 7 of the 18 (39%) prodromal subjects clinically progressed. Six subjects met formal criteria for schizophrenia spectrum disorders (3 with

schizophrenia, 2 with schizoaffective disorder, bipolar type, 1 with schizophreniform disorder), and 1 patient now meets the criteria for major depression with psychotic features.

In a primary analysis guided by the first study, we compared CBV values measured from the CA1 subfield, orbitofrontal cortex, and dorsolateral cortex between subjects who progressed with those who did not. The only between-group difference was observed in the CA1 subregion, where subjects who progressed were found to have significantly higher CBV values ($F_{1,17} = 6.8$; $P = .02$) (Figure 3A). In a secondary analysis, we expanded the focus to include all regions in which CBV was measured, and none were found to significantly distinguish between the groups.

Categorical analysis of baseline CBV data revealed that CA1 dysfunction predicted clinical progression with a positive predictive value of 71% and a negative predictive value of 82% from analysis of the resultant 2×2 table (Fisher exact $P = .05$).

DIFFERENTIAL CORRELATION OF CA1 DYSFUNCTION WITH CLINICAL SYMPTOMS

To minimize type I error, a multivariate regression model was used in primary analyses that included CBV values from the 3 regions identified in the first study: the CA1 subfield, the orbitofrontal cortex, and the dorsolateral prefrontal cortex. Additionally, to increase statistical reliability, we collapsed symptom scores when possible, thereby increasing the number of subjects included in the model. Then, in secondary analyses we performed additional simple correlations to better understand the source of the primary findings.

For positive symptoms, the combined positive rating scale was found to differentially correlate with CBV in the CA1 subfield and was associated with total positive symptoms ($\beta = .53$; $P = .01$). No association was observed between CBV in the orbitofrontal cortex or dorsolateral prefrontal cortex and positive symptoms (Figure 3C). Of the specific items, delusional severity was the positive symptom that had the strongest association with CA1 CBV ($\beta = .54$; $P = .003$). Because the 2 clinical groups might not be on a continuum, additional analyses were performed within each group. An association was found between CA1 CBV and delusions in both the schizophrenia ($\beta = .57$; $P = .01$) and the prodromal patient groups ($\beta = .58$; $P = .01$).

In contrast to positive symptoms, the scales for negative symptoms used for prodromal subjects and those with schizophrenia are incompatible, so we used summary scores of negative symptoms separately for each group. Of the patients with schizophrenia, no significant association was found with the summary of negative symptoms, although a trend was noted only for the CA1 subfield ($\beta = .61$; $P = .09$). Within the prodromal group, CBV in the CA1 subfield was significantly associated with total negative symptoms ($\beta = .59$; $P = .03$) as well as with the social dysfunction ($\beta = .58$; $P = .01$) and avolition items ($\beta = .6$; $P = .03$). Within this same regression model, dorsolateral prefrontal cortex CBV was also negatively associated with total negative symptoms in the prodromal group at a trend level ($\beta = -.47$; $P = .09$) and was negatively associated with the social withdrawal subscale ($\beta = -.73$; $P = .005$).

NO ASSOCIATION BETWEEN CA1 DYSFUNCTION AND MEDICATION USE

Only 1 of 7 subjects who clinically progressed received antipsychotic medications at baseline, suggesting that our CA1 CBV findings were not confounded by antidopaminergic agents. Supporting this interpretation, comparing mean CBV values of the 3 prodromal subjects who were taking antipsychotic medications with those of the 15 subjects who were not revealed no significant difference in CA1 CBV ($t = -0.68$; $P = .51$) (Figure 4). Four of the 7 subjects who clinically progressed received antidepressant medications at baseline. Antidepressant use (Fisher exact $P = .67$) and antipsychotic use (Fisher exact $P = .67$) were not associated with conversion status. Finally, an analysis comparing the mean CBV values of the 10 prodromal

subjects who were taking antidepressant medications with those of the 8 who were not revealed no significant difference in CA1 CBV ($t = -0.47$; $P = .65$) (Figure 4).

To further explore this issue in an experimental setting, we performed an experiment in which 5 C57/B6 mice received the antipsychotic agent risperidone (0.75 mg/kg, twice per day by oral gavage) for 3 weeks and 5 mice received vehicle control. Hippocampal CBV maps (Figure 5) were generated before and after drug administration and a repeated-measures ANOVA revealed no drug effect in any hippocampal subregion, including the CA1 subfield ($F = 0.50$; $P = .50$) (Figure 5).

COMMENT

Our main finding is that dysfunction in the CA1 subfield of the hippocampal formation best fulfilled the clinical criteria for a brain site differentially targeted by schizophrenia and related psychotic disorders: (1) it is present in the established diagnosis of schizophrenia; (2) it selectively predicts clinical progression; and (3) it is differentially associated with both positive and negative symptoms of psychosis. The observed pattern of dysfunction found in our study, characterized by abnormal elevations of CBV, is suggestive of a basal hypermetabolic state^{15,30} in the hippocampus in schizophrenia. Basal metabolic increases in the medial temporal lobe or hippocampal formation that are associated with symptoms of psychosis have been shown in most published single-photon emission computed tomography^{31,32} and positron emission tomography-based studies of schizophrenia using basal cerebral blood flow,^{33–35} a correlate of CBV,³⁶ consistent with our findings. Nevertheless, because of suboptimal spatial resolution, imaging approaches using cerebral blood flow have shown global medial temporal or hippocampal hypermetabolism but cannot pinpoint defects to specific hippocampal subregions.

In prodromal research, baseline predictors of transition to psychosis have not yet been shown convincingly with existing methodologies. Although the volume of the hippocampus appears to be decreased compared with controls at baseline,^{37–41} it has not predicted transition to psychosis in 3 of 5 published studies. In one study that originally predicted transition,³⁷ voxel-based morphometry methodology was used, and a study of this expanded sample using region-of-interest methodology did not replicate the earlier finding.⁴² By contrast, longitudinal study of high-risk patients has shown progressive reduction of medial temporal lobe volumes in patients whose psychosis became exacerbated over time.³⁷ N-acetyl-aspartate levels in the hippocampus, as assessed by magnetic resonance spectroscopy, are equivalent to those of controls and are not known to predict psychosis.⁴³ Prefrontal volume contraction has been associated with the onset of psychosis but has not predicted psychosis at baseline in a large clinical high-risk sample.⁴⁴ Among patients at genetically high risk from the Edinburgh sample⁴⁵ (eg, with a first-degree relative with a psychotic disorder), predictors of transition to psychosis have been found in prefrontal regions and have included increased prefrontal gyrification. Less inferior frontal gray matter at baseline was shown in ultra-high-risk individuals who transitioned to psychosis in one sample,⁴⁰ while decreased right prefrontal gray matter from baseline to transition to psychosis has been shown in a separate sample using longitudinal methods.⁴⁴

Previous studies have suggested that the CA1 subfield of the hippocampal formation might be involved in psychotic illness. In particular, studies by Benes and colleagues^{46–48} have relied on observed postmortem changes in interneurons to predict increased excitation in the hippocampal formation and, based on properties of the hippocampal trisynaptic circuit, have hypothesized that the CA1 subfield might exhibit the greatest increase in excitation.⁴⁹ However, as described,⁴⁹ establishing the precise location and functional alterations in the hippocampal formation must be empirically determined.

Further studies rely on the observation that N-methyl-D-aspartate antagonists phenocopy many key clinical features of schizophrenia.⁵⁰ Several models of N-methyl-D-aspartate receptor hypofunction predict that the locus of this effect should occur predominately in the CA1 subfield of the hippocampal formation^{51,52} as well as affect interneuron function.⁵³ Nonetheless, these models have not excluded the importance of other hippocampal subregions. More importantly, whereas one model predicts that N-methyl-D-aspartate antagonists would reduce activity of inhibitory interneurons, leading to increased excitation,⁵¹ other models predict that N-methyl-D-aspartate antagonists act on primary neurons, leading to decreased CA1 excitation.⁵² Thus, there is disagreement as to whether this subfield exhibits an increase or decrease in activity and whether other hippocampal subregions might also be involved.

Brambilla et al⁵⁴ and Loeber et al⁵⁵ have performed CBV estimates of the hemisphere and cerebellum in patients with established schizophrenia and found evidence of hemispheric decreases in CBV and cerebellum increases in CBV. Because they used different methods to obtain their estimates of CBV, normalized their results using differing methodologies, and chose differing regions of interest, it is difficult to draw direct comparisons of how the present study relates to the prior CBV studies.

Our study is the first to apply high-resolution functional imaging to prodromal subjects, a newly developed clinical category that, although etiologically heterogeneous, is enriched with subjects in the early stages of schizophrenia and related psychotic disorders. The results demonstrate that CA1 dysfunction is an early and selective defect that predicts progression to psychosis, which, by virtue of the characteristics of the prodromal patient sample, is not confounded by illness duration or antipsychotic treatment effects. As noted, subjects who clinically progressed had schizophrenia, but also schizoaffective disorder and major depression with psychotic features. Future studies imaging a larger group of prodromal subjects are required to clarify the question of the diagnostic utility of CA1 subfield CBV, despite its remarkably high predictive power in this small sample. At the same time, the selectivity and statistical strength of the findings indicate that CA1 dysfunction is at least 1 primary defect in schizophrenia. This interpretation is supported by the associational analyses showing that the CA1 subfield consistency correlates with clinical symptoms in patients with documented schizophrenia as well as in prodromal subjects. Although each of the 3 imaging analyses—mapping disease-selective dysfunction, predicting progression, and associating dysfunction with symptoms—has limitations, as a composite they provide strong evidence that the CA1 subfield is a brain site differentially targeted in schizophrenia and related disorders.

Our findings support the hypothesis that psychosis is characterized by abnormal excitation of hippocampal afferents linked to increases in synaptic glutamate. Besides evidence from spectroscopy studies investigating patients with schizophrenia,⁵⁶ this view is supported by animal models showing how stimulation of hippocampal afferents results in elevated cell population dopamine activity.^{57–59} Moreover, a recent drug study has shown clinical efficacy in patients using an agonist of the metabotropic glutamate 2/3 receptors, which causes a decrease in glutamate release.⁶⁰ Future animal or postmortem studies are required to isolate the molecular and cellular mechanisms that underlie CA1 subfield dysfunction, perhaps by affecting mechanisms of glutamate regulation in the hippocampal circuit.

Our study has important limitations. First, although large for an functional magnetic resonance imaging study, the sample size could be larger, particularly to assess the diagnostic utility of the findings. Second, though we are confident that inclusion of a prodromal group and an animal treatment study provides evidence that antipsychotic treatment did not confound our results (Medoff et al³⁵ shows normalization of hippocampal hypermetabolism with treatment), we recognize that testing medication-free subjects with first-episode psychosis is a priority for future research to more definitively establish our subregional findings. Third, we recognize

that user-guided region-of-interest techniques are imperfect; however, there are presently no automated methods available to investigate hippocampal subregions.

At a phenomenological level, our findings raise questions regarding why CA1 hypermetabolism would be so tightly linked to symptoms of the disease. In this regard, it is interesting to note that the anterior CA1 subfield and the subiculum monosynaptically connect with a number of outflow sites implicated in schizophrenia,⁶¹ including the orbitofrontal cortex.⁶² Thus, it is interesting to postulate that CA1 hypermetabolism may be driving dysfunction in other brain regions in the established illness. By combining functional magnetic resonance imaging techniques with other imaging modalities such as positron emission tomography that can assess dopamine release, and by applying these techniques to a large number of prodromal subjects followed up longitudinally, it is now possible to test these circuit-based hypotheses in living subjects.

Acknowledgments

Funding/Support: This study was supported in part by National Institutes of health federal grants AG025161 (Dr Small), K24 MH01699 (Dr Malaspina), and K23MH066279 (Dr Corcoran); National Alliance for Research on Schizophrenia and Depression (Drs Corcoran and Schobel); and the Irving Institute for Clinical and Translational Research (Drs Corcoran and Schobel).

References

- Shenton ME, Dickey CC, Frumin M, McCarley RW. A review of MRI findings in schizophrenia. *Schizophr Res* 2001;49(1-2):1-52. [PubMed: 11343862]
- Zhao X, Lein ES, He A, Smith SC, Aston C, Gage FH. Transcriptional profiling reveals strict boundaries between hippocampal subregions. *J Comp Neurol* 2001;441(3):187-196. [PubMed: 11745644]
- Small SA, Nava AS, Perera GM, Delapaz R, Stern Y. Evaluating the function of hippocampal subregions with high-resolution MRI in Alzheimer's disease and aging. *Microsc Res Tech* 2000;51(1):101-108. [PubMed: 11002358]
- Harrison PJ. The neuropathology of schizophrenia: a critical review of the data and their interpretation. *Brain* 1999;122(pt 4):593-624. [PubMed: 10219775]
- Yung AR, McGorry PD. The prodromal phase of first-episode psychosis: past and current conceptualizations. *Schizophr Bull* 1996;22(2):353-370. [PubMed: 8782291]
- Yung AR, Phillips LJ, Yuen HP, McGorry PD. Risk factors for psychosis in an ultra high-risk group: psychopathology and clinical features. *Schizophr Res* 2004;67(2-3):131-142. [PubMed: 14984872]
- Klosterkötter J, Hellmich M, Steinmeyer EM, Schultze-Lutter F. Diagnosing schizophrenia in the initial prodromal phase. *Arch Gen Psychiatry* 2001;58(2):158-164. [PubMed: 11177117]
- Cannon TD, Cadenhead K, Cornblatt B, Woods SW, Addington J, Walker E, Seidman LJ, Perkins D, Tsuang M, McGlashan T, Heinssen R. Prediction of psychosis in youth at high clinical risk: a multisite longitudinal study in North America. *Arch Gen Psychiatry* 2008;65(1):28-37. [PubMed: 18180426]
- Perlmutter JS, Powers WJ, Herscovitch P, Fox PT, Raichle ME. Regional asymmetries of cerebral blood flow, blood volume, and oxygen utilization and extraction in normal subjects. *J Cereb Blood Flow Metab* 1987;7(1):64-67. [PubMed: 3492507]
- van Zijl PC, Eleff SM, Ulatowski JA, Oja JM, Ulug AM, Traystman RJ, Kauppinen RA. Quantitative assessment of blood flow, blood volume and blood oxygenation effects in functional magnetic resonance imaging. *Nat Med* 1998;4(2):159-167. [PubMed: 9461188]
- Mandeville JB, Jenkins BG, Kosofsky BE, Moskowitz MA, Rosen BR, Marota JJ. Regional sensitivity and coupling of BOLD and CBV changes during stimulation of rat brain. *Magn Reson Med* 2001;45(3):443-447. [PubMed: 11241702]
- Buxton RB, Uludag K, Dubowitz DJ, Liu TT. Modeling the hemodynamic response to brain activation. *Neuroimage* 2004;23(suppl 1):S220-S233. [PubMed: 15501093]

13. Small SA, Wu EX, Bartsch D, Perera GM, Lacefield CO, DeLaPaz R, Mayeux R, Stern Y, Kandel ER. Imaging physiologic dysfunction of individual hippocampal subregions in humans and genetically modified mice. *Neuron* 2000;28(3):653–664. [PubMed: 11163257]
14. Lin W, Celik A, Paczynski RP. Regional cerebral blood volume: a comparison of the dynamic imaging and the steady state methods. *J Magn Reson Imaging* 1999;9(1):44–52. [PubMed: 10030649]
15. González RG, Fischman AJ, Guimaraes AR, Carr CA, Stern CE, Halpern EF, Growdon JH, Rosen BR. Functional MR in the evaluation of dementia: correlation of abnormal dynamic cerebral blood volume measurements with changes in cerebral metabolism on positron emission tomography with fludeoxyglucose F 18. *AJNR Am J Neuroradiol* 1995;16(9):1763–1770. [PubMed: 8693972]
16. Moreno H, Wu WE, Lee T, Brickman A, Mayeux R, Brown TR, Small SA. Imaging the abeta-related neurotoxicity of Alzheimer disease. *Arch Neurol* 2007;64 (10):1467–1477. [PubMed: 17923630]
17. Small SA, Chawla MK, Buonocore M, Rapp PR, Barnes CA. Imaging correlates of brain function in monkeys and rats isolates a hippocampal subregion differentially vulnerable to aging. *Proc Natl Acad Sci U S A* 2004;101(18):7181–7186. [PubMed: 15118105]
18. Moreno H, Hua F, Brown T, Small S. Longitudinal mapping of mouse cerebral blood volume with MRI. *NMR Biomed* 2006;19(5):535–543. [PubMed: 16552789]
19. Chen YJ, Johnson MA, Lieberman MD, Goodchild RE, Schobel S, Lewandowski N, Rosoklija G, Liu RC, Gingrich JA, Small S, Moore H, Dwork AJ, Talmage DA, Role LW. Type III neuregulin-1 is required for normal sensorimotor gating, memory-related behaviors, and corticostriatal circuit components. *J Neurosci* 2008;28(27):6872–6883. [PubMed: 18596162]
20. Nurnberger JI Jr, Blehar MC, Kaufmann CA, York-Cooler C, Simpson SG, Harkavy-Friedman J, Severe JB, Malaspina D, Reich T. Diagnostic interview for genetic studies: rationale, unique features, and training: NIMH Genetics Initiative. *Arch Gen Psychiatry* 1994;51(11):849–859. discussion 863–844. [PubMed: 7944874]
21. Miller TJ, McGlashan TH, Rosen JL, Cadenhead K, Cannon T, Ventura J, McFarlane W, Perkins DO, Pearlson GD, Woods SW. Prodromal assessment with the structured interview for prodromal syndromes and the scale of prodromal symptoms. *Schizophr Bull* 2003;29(4):703–715. [PubMed: 14989408]
22. Chambers WJ, Puig-Antich J, Hirsch M, Paez P, Ambrosini PJ, Tabrizi MA, Davies M. The assessment of affective disorders in children and adolescents by semi-structured interview: test-retest reliability of the schedule for affective disorders and schizophrenia for school-age children, present episode version. *Arch Gen Psychiatry* 1985;42(7):696–702. [PubMed: 4015311]
23. Kay SR, Fiszbein A, Opler LA. The positive and negative syndrome scale (PANSS) for schizophrenia. *Schizophr Bull* 1987;13(2):261–276. [PubMed: 3616518]
24. Pereira AC, Huddleston DE, Brickman AM, Sosunov AA, Hen R, McKhann GM, Sloan R, Gage FH, Brown TR, Small SA. An in vivo correlate of exercise-induced neurogenesis in the adult dentate gyrus. *Proc Natl Acad Sci U S A* 2007;104 (13):5638–5643. [PubMed: 17374720]
25. Rajkowska G, Goldman-Rakic PS. Cytoarchitectonic definition of prefrontal areas in the normal human cortex I: remapping of areas 9 and 46 using quantitative criteria. *Cereb Cortex* 1995;5(4):307–322. [PubMed: 7580124]
26. Mai, JK.; Assheuer, J.; Paxinos, G. *The Atlas of the Human Brain*. Vol. 3. San Diego, CA: Academic Press; 1997.
27. Etkin A, Klemenhagen KC, Dudman JT, Rogan MT, Hen R, Kandel ER, Hirsch J. Individual differences in trait anxiety predict the response of the basolateral amygdala to unconsciously processed fearful faces. *Neuron* 2004;44(6):1043–1055. [PubMed: 15603746]
28. Wadenberg ML, Soliman A, VanderSpek SC, Kapur S. Dopamine D(2) receptor occupancy is a common mechanism underlying animal models of antipsychotics and their clinical effects. *Neuropsychopharmacology* 2001;25(5):633–641. [PubMed: 11682246]
29. Barth VN, Chernet E, Martin LJ, Need AB, Rash KS, Morin M, Phebus LA. Comparison of rat dopamine D2 receptor occupancy for a series of antipsychotic drugs measured using radiolabeled or nonlabeled raclopride tracer. *Life Sci* 2006;78(26):3007–3012. [PubMed: 16434058]
30. Gado MH, Phelps ME, Hoffman EJ, Raichle ME. Changes in cerebral blood volume and vascular mean transit time during induced cerebral seizures. *Radiology* 1976;121(1):105–109. [PubMed: 822474]

31. Malaspina D, Harkavy-Friedman J, Corcoran C, Mujica-Parodi L, Printz D, Gorman JM, Van Heertum R. Resting neural activity distinguishes subgroups of schizophrenia patients. *Biol Psychiatry* 2004;56(12):931–937. [PubMed: 15601602]
32. Kawasaki Y, Suzuki M, Maeda Y, Urata K, Yamaguchi N, Matsuda H, Hisada K, Suzuki M, Takashima T. Regional cerebral blood flow in patients with schizophrenia. *Eur Arch Psychiatry Clin Neurosci* 1992;241(4):195–200. [PubMed: 1576174]
33. Friston KJ, Liddle PF, Frith CD, Hirsch SR, Frackowiak RS. The left medial temporal region and schizophrenia: a PET study. *Brain* 1992;115(pt 2):367–382. [PubMed: 1606474]
34. Heckers S, Rauch SL, Goff D, Savage CR, Schacter DL, Fischman AJ, Alpert NM. Impaired recruitment of the hippocampus during conscious recollection in schizophrenia. *Nat Neurosci* 1998;1(4):318–323. [PubMed: 10195166]
35. Medoff DR, Holcomb HH, Lahti AC, Tamminga CA. Probing the human hippocampus using rCBF: contrasts in schizophrenia. *Hippocampus* 2001;11(5):543–550. [PubMed: 11732707]
36. Grubb RL Jr, Raichle ME, Eichling JO, Ter-Pogossian MM. The effects of changes in PaCO₂ on cerebral blood volume, blood flow, and vascular mean transit time. *Stroke* 1974;5(5):630–639. [PubMed: 4472361]
37. Pantelis C, Velakoulis D, McGorry PD, Wood SJ, Suckling J, Phillips LJ, Yung AR, Bullmore ET, Brewer W, Soulsby B, Desmond P, McGuire PK. Neuroanatomical abnormalities before and after onset of psychosis: a cross-sectional and longitudinal MRI comparison. *Lancet* 2003;361(9354):281–288. [PubMed: 12559861]
38. Job DE, Whalley HC, Johnstone EC, Lawrie SM. Grey matter changes over time in high risk subjects developing schizophrenia. *Neuroimage* 2005;25(4):1023–1030. [PubMed: 15850721]
39. Phillips LJ, Velakoulis D, Pantelis C, Wood S, Yuen HP, Yung AR, Desmond P, Brewer W, McGorry PD. Non-reduction in hippocampal volume is associated with higher risk of psychosis. *Schizophr Res* 2002;58(2–3):145–158. [PubMed: 12409154]
40. Borgwardt SJ, Riecher-Rossler A, Dazzan P, Chitnis X, Aston J, Drewe M, Gschwandtner U, Haller S, Pfluger M, Rechssteiner E, D'Souza M, Stieglitz RD, Radu EW, McGuire PK. Regional gray matter volume abnormalities in the at risk mental state. *Biol Psychiatry* 2007;61(10):1148–1156. [PubMed: 17098213]
41. Hurlmann R, Jessen F, Wagner M, Frommann I, Ruhrmann S, Brockhaus A, Pickler H, Scheef L, Block W, Schild HH, Moller-Hartmann W, Krug B, Falkai P, Klosterkötter J, Maier W. Interrelated neuropsychological and anatomical evidence of hippocampal pathology in the at-risk mental state. *Psychol Med* 2008;38(6):843–851. [PubMed: 18387213]
42. Velakoulis D, Wood SJ, Wong MT, McGorry PD, Yung A, Phillips L, Smith D, Brewer W, Proffitt T, Desmond P, Pantelis C. Hippocampal and amygdala volumes according to psychosis stage and diagnosis: a magnetic resonance imaging study of chronic schizophrenia, first-episode psychosis, and ultra-high-risk individuals. *Arch Gen Psychiatry* 2006;63(2):139–149. [PubMed: 16461856]
43. Wood SJ, Berger G, Velakoulis D, Phillips LJ, McGorry PD, Yung AR, Desmond P, Pantelis C. Proton magnetic resonance spectroscopy in first episode psychosis and ultra high-risk individuals. *Schizophr Bull* 2003;29(4):831–843. [PubMed: 14989417]
44. Sun D, Phillips L, Velakoulis D, Yung A, McGorry PD, Wood SJ, van Erp TG, Thompson PM, Toga AW, Cannon TD, Pantelis C. Progressive brain structural changes mapped as psychosis develops in 'at risk' individuals. *Schizophr Res* 2009;108(1–3):85–92. [PubMed: 19138834]
45. Harris JM, Moorhead TW, Miller P, McIntosh AM, Bonnici HM, Owens DG, Johnstone EC, Lawrie SM. Increased prefrontal gyrification in a large high-risk cohort characterizes those who develop schizophrenia and reflects abnormal prefrontal development. *Biol Psychiatry* 2007;62(7):722–729. [PubMed: 17509536]
46. Benes FM, Kwok EW, Vincent SL, Todtenkopf MS. A reduction of nonpyramidal cells in sector CA2 of schizophrenics and manic depressives. *Biol Psychiatry* 1998;44(2):88–97. [PubMed: 9646890]
47. Benes FM, Lim B, Matzilevich D, Walsh JP, Subburaju S, Minns M. Regulation of the GABA cell phenotype in hippocampus of schizophrenics and bipolars. *Proc Natl Acad Sci U S A* 2007;104(24):10164–10169. [PubMed: 17553960]

48. Heckers S, Stone D, Walsh J, Shick J, Koul P, Benes FM. Differential hippocampal expression of glutamic acid decarboxylase 65 and 67 messenger RNA in bipolar disorder and schizophrenia. *Arch Gen Psychiatry* 2002;59(6):521–529. [PubMed: 12044194]
49. Benes FM. Evidence for altered trisynaptic circuitry in schizophrenic hippocampus. *Biol Psychiatry* 1999;46(5):589–599. [PubMed: 10472413]
50. Javitt DC. Glutamate and schizophrenia: phencyclidine, N-methyl-d-aspartate receptors, and dopamine-glutamate interactions. *Int Rev Neurobiol* 2007;78:69–108. [PubMed: 17349858]
51. Greene R. Circuit analysis of NMDAR hypofunction in the hippocampus, in vitro, and psychosis of schizophrenia. *Hippocampus* 2001;11(5):569–577. [PubMed: 11732709]
52. Siekmeier PJ, Hasselmo ME, Howard MW, Coyle J. Modeling of context-dependent retrieval in hippocampal region CA1: implications for cognitive function in schizophrenia. *Schizophr Res* 2007;89(1–3):177–190. [PubMed: 17055702]
53. Braun I, Genius J, Grunze H, Bender A, Moller HJ, Rujescu D. Alterations of hippocampal and prefrontal GABAergic interneurons in an animal model of psychosis induced by NMDA receptor antagonism. *Schizophr Res* 2007;97(1–3):254–263. [PubMed: 17601703]
54. Brambilla P, Cerini R, Fabene PF, Andreone N, Rambaldelli G, Farace P, Versace A, Perlini C, Pelizza L, Gasparini A, Gatti R, Bellani M, Dusi N, Barbui C, Nose M, Tournikioti K, Sbarbati A, Tansella M. Assessment of cerebral blood volume in schizophrenia. *J Psychiatr Res* 2007;41(6):502–510. [PubMed: 16698038]
55. Loeber RT, Sherwood AR, Renshaw PF, Cohen BM, Yurgelun-Todd DA. Differences in cerebellar blood volume in schizophrenia and bipolar disorder. *Schizophr Res* 1999;37(1):81–89. [PubMed: 10227110]
56. van Elst LT, Valerius G, Buchert M, Thiel T, Rusch N, Bubl E, Hennig J, Ebert D, Olbrich HM. Increased prefrontal and hippocampal glutamate concentration in schizophrenia. *Biol Psychiatry* 2005;58(9):724–730. [PubMed: 16018980]
57. Legault M, Wise RA. Injections of N-methyl-D-aspartate into the ventral hippocampus increase extracellular dopamine in the ventral tegmental area and nucleus accumbens. *Synapse* 1999;31(4):241–249. [PubMed: 10051104]
58. Floresco SB, Todd CL, Grace AA. Glutamatergic afferents from the hippocampus to the nucleus accumbens regulate activity of ventral tegmental area dopamine neurons. *J Neurosci* 2001;21(13):4915–4922. [PubMed: 11425919]
59. Lodge DJ, Grace AA. Aberrant hippocampal activity underlies the dopamine dysregulation in an animal model of schizophrenia. *J Neurosci* 2007;27(42):11424–11430. [PubMed: 17942737]
60. Patil ST, Zhang L, Martenyi F, Lowe SL, Jackson KA, Andreev BV, Avedisova AS, Bardenstein LM, Gurovich IY, Morozova MA, Mosolov SN, Neznanov NG, Reznik AM, Smulevich AB, Tochilov VA, Johnson BG, Monn JA, Schoepp DD. Activation of mGlu2/3 receptors as a new approach to treat schizophrenia: a randomized phase 2 clinical trial. *Nat Med* 2007;13(9):1102–1107. [PubMed: 17767166]
61. Rosene DL, Van Hoesen GW. Hippocampal efferents reach widespread areas of cerebral cortex and amygdala in the rhesus monkey. *Science* 1977;198(4314):315–317. [PubMed: 410102]
62. Homayoun H, Moghaddam B. Orbitofrontal cortex neurons as a common target for classic and glutamatergic antipsychotic drugs. *Proc Natl Acad Sci U S A* 2008;105(46):18041–18046. [PubMed: 19004793]

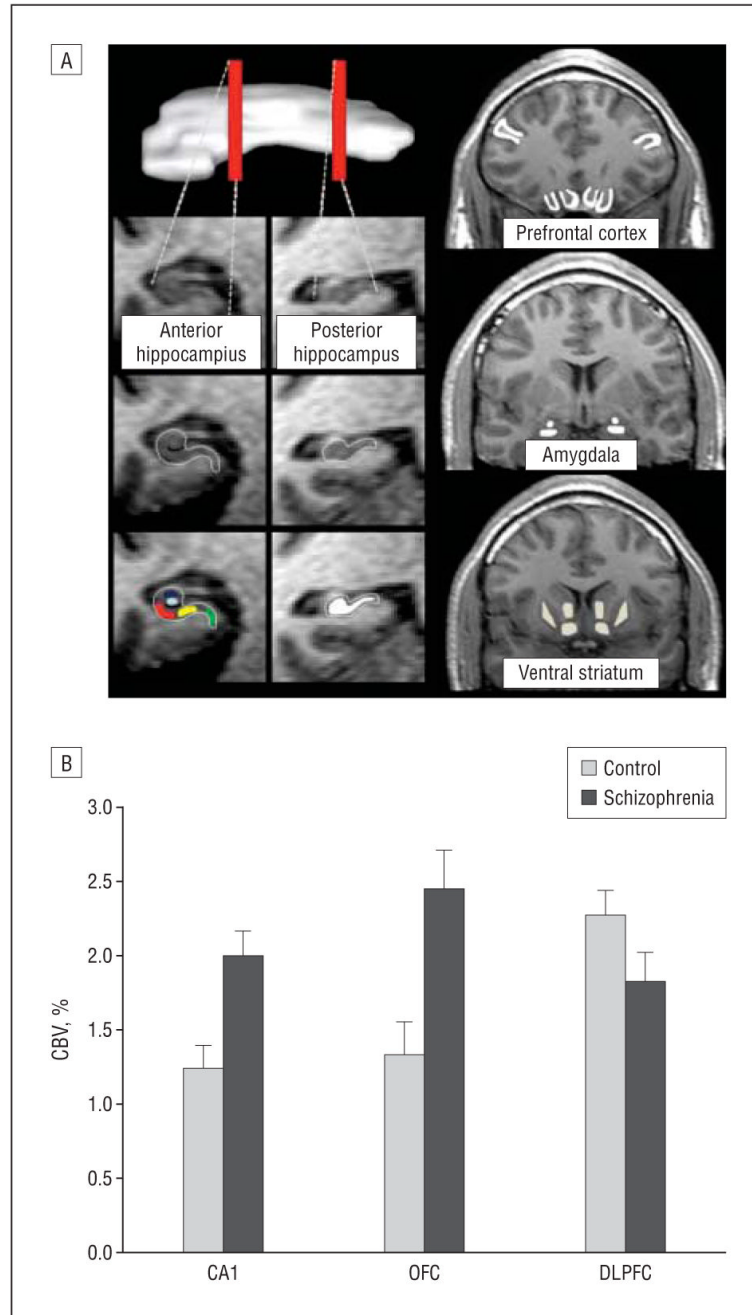


Figure 1.

Dysfunction in multiple regions in brain areas implicated in schizophrenia. A, Using high-resolution T1-weighted images, resting-state cerebral blood volume (CBV) mapping is a variant of functional magnetic resonance imaging that, as shown, can visualize the anterior and posterior hippocampus (a superior oblique view of the hippocampus is shown on the top left); subregions within the anterior hippocampus (green indicates entorhinal cortex; light blue, dentate gyrus; dark blue, CA3; red, CA1; yellow, subiculum); the posterior hippocampus (white); the frontal lobe in coronal section (inferior regions indicate orbitofrontal cortex and gyrus rectus; superior-lateral regions, dorsolateral cortex); the basal ganglia (medial regions indicate ventral caudate and nucleus accumbens; lateral regions, ventral putamen); and the

amygdala (superior region indicates dorsal amygdala; inferior, basolateral amygdala). B, An increase in CBV between the 2 groups (control, schizophrenia) was observed selectively for the CA1 subfield of the hippocampal formation and the orbitofrontal cortex (OFC), while a CBV decrease was observed in the dorsolateral prefrontal cortex (DLPFC).

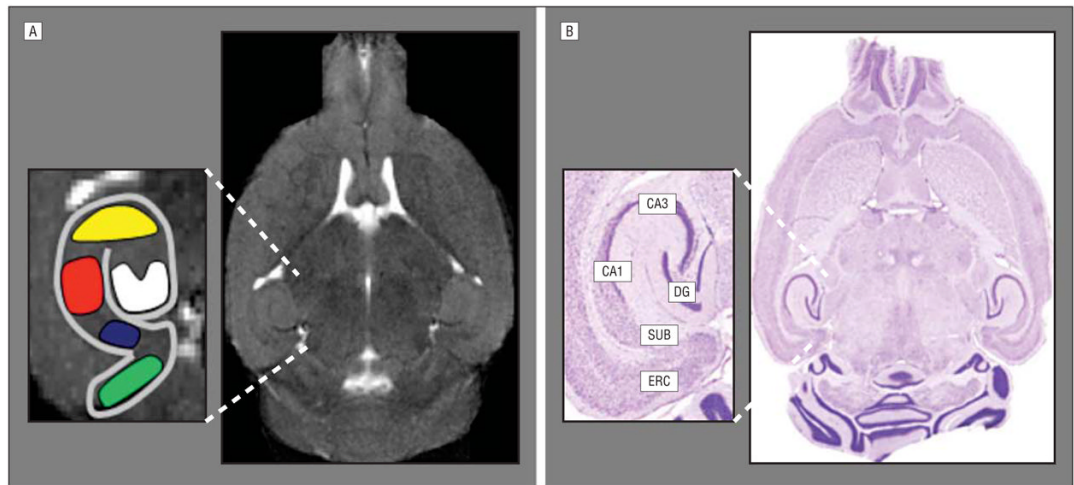


Figure 2.

Resting-state cerebral blood volume (CBV) mapping in mice. A, A horizontal high-resolution T2-weighted magnetic resonance image is generated with a high-field 9.4-T scanner and used to obtain resting-state CBV maps of the mouse hippocampal formation. Green indicates entorhinal cortex; white, dentate gyrus; yellow, CA3; red, CA1; dark blue, subiculum. B, A horizontal brain section with Nissl staining shows the correspondence between the magnetic resonance imaging scan and the histological anatomy of the individual hippocampal subregions. ERC indicates entorhinal cortex; SUB, subiculum; CA1, CA1 subfield; CA3, CA3 subfield; DG, dentate gyrus.

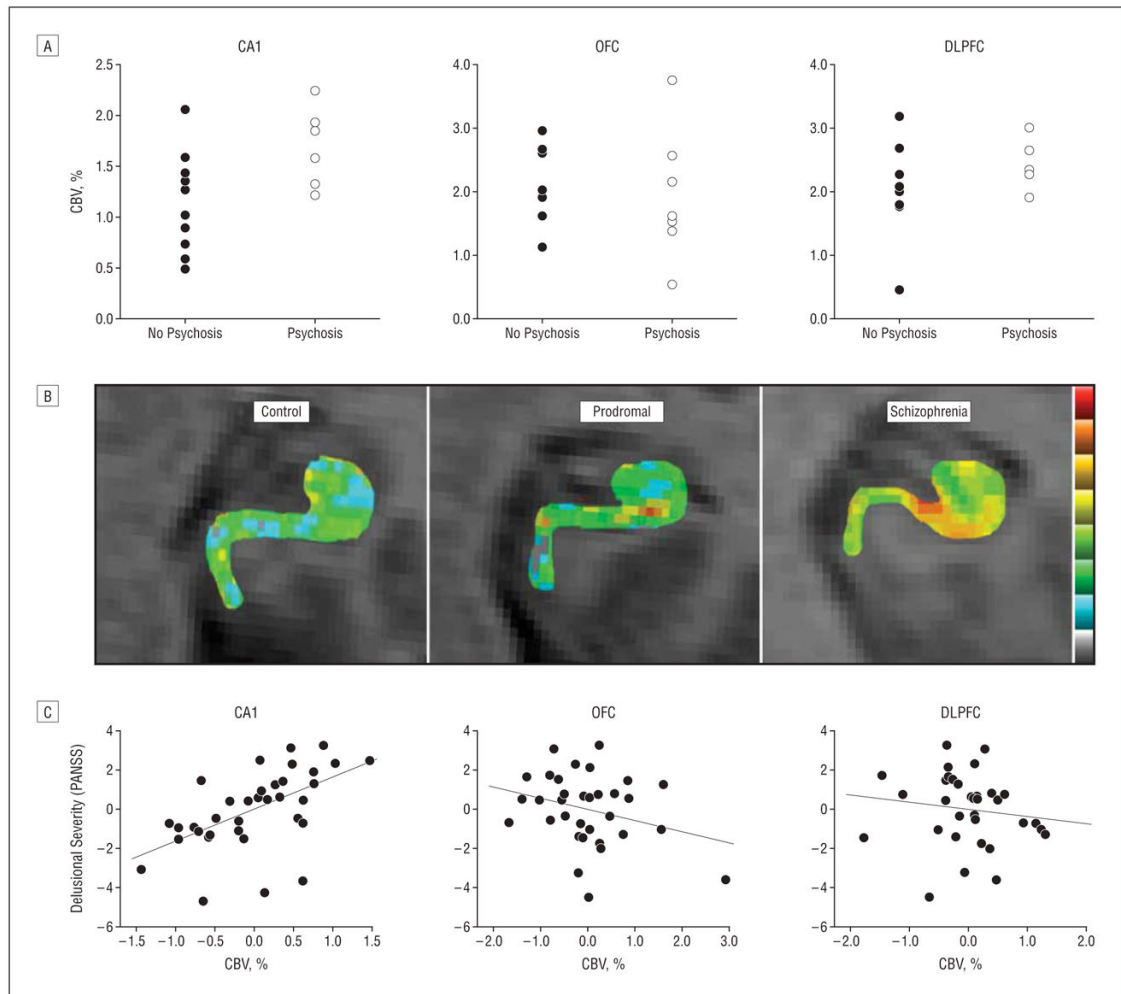


Figure 3.

The CA1 subfield is a site of dysfunction selectively associated with clinical features. A, Cerebral blood volume (CBV) measured in the CA1 subfield, but not the orbitofrontal cortex (OFC) or dorsolateral prefrontal cortex (DLPFC), was significantly elevated at baseline, comparing the prodromal subjects who clinically progressed to psychosis with those who did not. B, Individual CBV maps of the hippocampal formation are shown for a healthy control, a prodromal subject, and a patient with schizophrenia. The CBV maps are color coded such that warmer colors reflect higher CBV values. Higher CBV was observed in the CA1 subfield of the prodromal subject, and higher CBV was observed in the CA1 and subiculum in the patient with schizophrenia. C, CA1 CBV, but not OFC or DLPFC CBV correlated with positive symptoms, in particular, delusional severity. PANSS indicates Positive and Negative Symptom Scale.

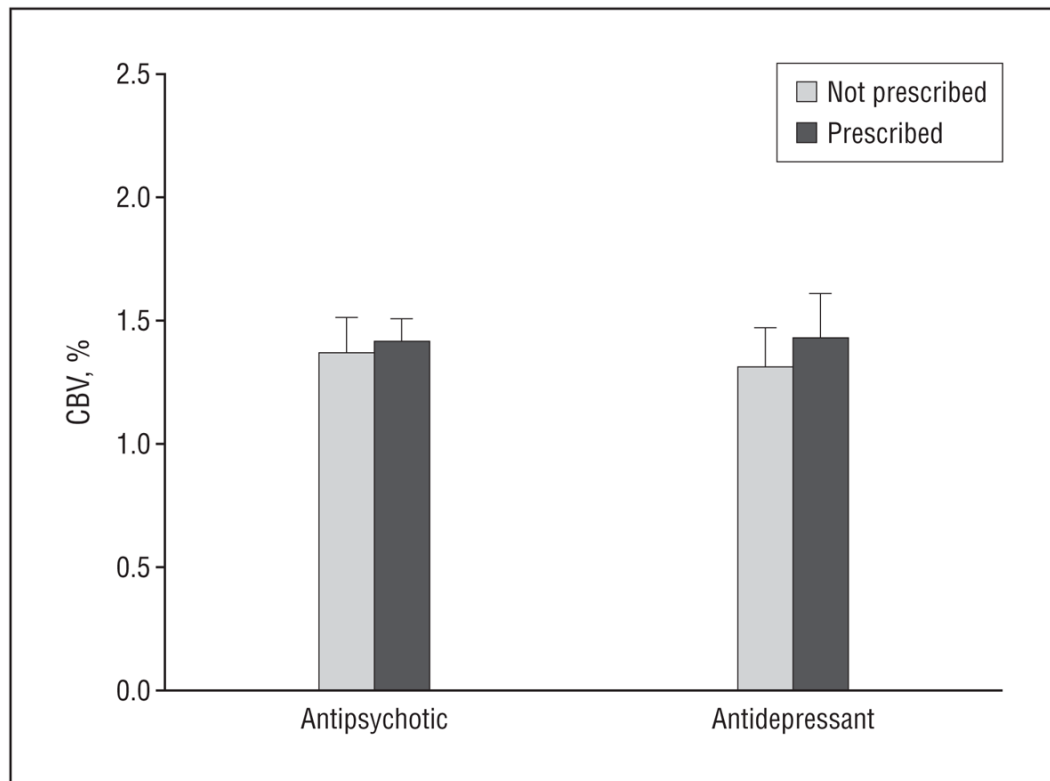


Figure 4. Cerebral blood volume (CBV) measured in the CA1 subfield compares the prodromal subjects who were prescribed antidepressant or antipsychotic drugs with those who were not.

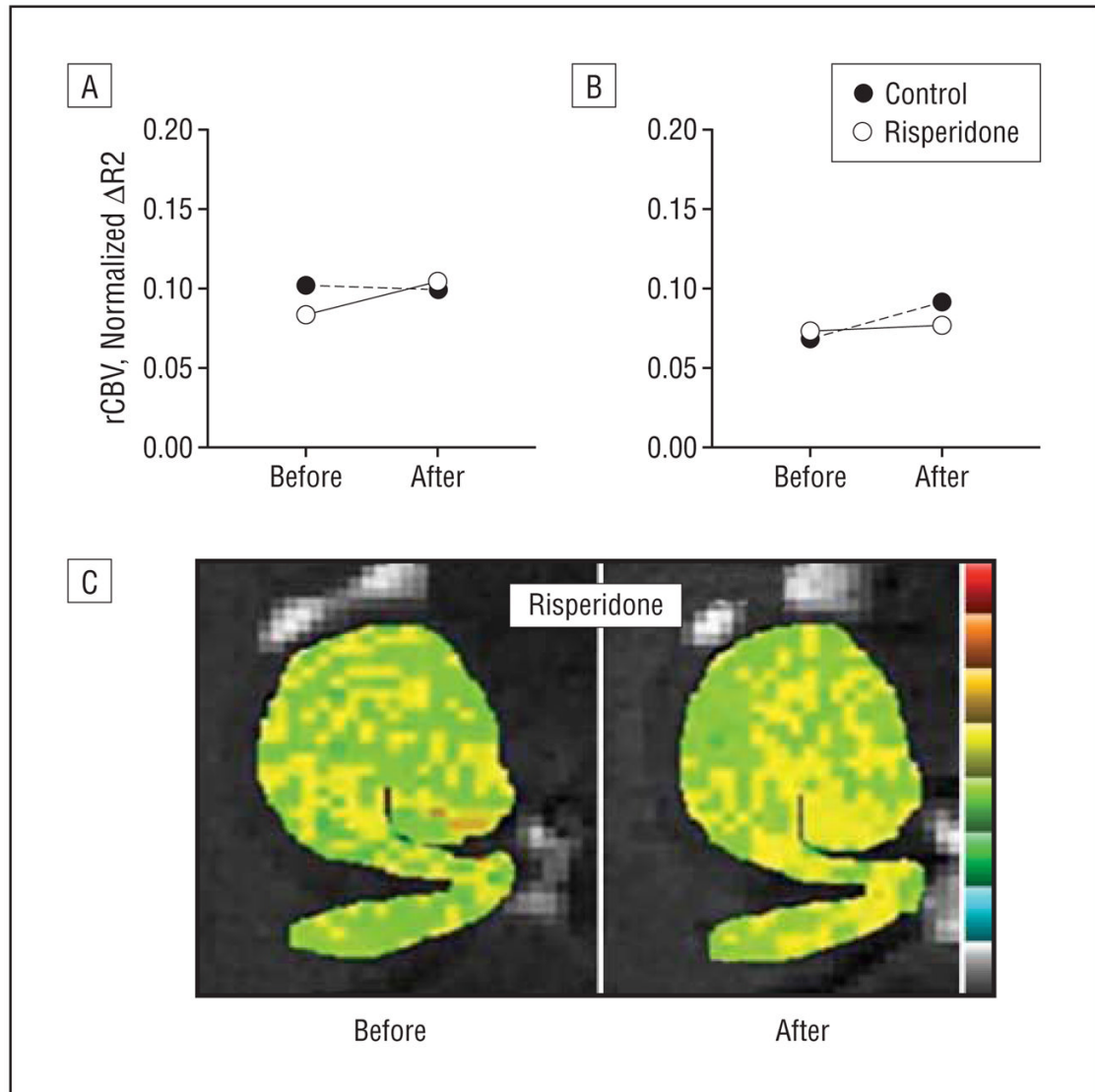


Figure 5. Relative cerebral blood volume (rCBV) maps were generated in mice before and after long-term administration of the dopamine blocking agent risperidone. Risperidone had no effect on hippocampal CBV, as shown for averaged group data measured in the CA1 subfield (A) and entorhinal cortex (B) as well as a hippocampal CBV map from a single mouse before and after receiving risperidone (C).

Table 1

Subject Demographics

| Category | No./Total (%) | | | Control vs Schizophrenia |
|---------------------------|---------------|-----------------|---------------|---------------------------|
| | Control | Ultra-High-Risk | Schizophrenia | |
| Subjects | 18 | 18 | 18 | |
| Mean (SD) age, y | 31.1 (8.5) | 18.8 (3.7) | 33.1 (7.5) | $t_{34} = -.88, P = .39$ |
| Men:Women | 13:5 | 17:1 | 13:5 | $\chi^2 = 3.7; P = .16^a$ |
| Education, y | 15.8 (3.6) | 12.6 (2.6) | 14.1 (2.2) | $t_{34} = 1.6, P = .12$ |
| Duration of illness, y | NA | NA | 10.5 (7.5) | NA |
| Total PANSS positive | NA | NA | 16.6 (8.6) | NA |
| Total PANSS negative | NA | NA | 14.2 (5.8) | NA |
| Total SOPS positive | NA | 11.4 (3.1) | NA | NA |
| Total SOPS negative | NA | 11.2 (5.1) | NA | NA |
| Antipsychotic treatment | 0/18 | 3/18 | 17/18 | NA |
| Antidepressant treatment | 0/18 | 10/18 | 5/18 | NA |
| Mood stabilizer treatment | 0/18 | 2/18 | 5/18 | NA |

Abbreviations: NA, not applicable; PANSS, Positive and Negative Symptom Scale; SOPS, Scale of Prodromal Symptoms.

^aIncludes ultra-high-risk group.

Table 2
Cerebral Blood Volumes by Subregion

| Subregion | Mean (SD) | | |
|--------------------------------|-------------|-----------------|--------------------------|
| | Control | Ultra-High-Risk | Schizophrenia |
| Anterior hippocampus | | | |
| Entorhinal cortex | 1.56 (0.84) | 1.41 (0.92) | 1.29 (1.03) |
| Subiculum | 1.76 (0.88) | 1.60 (0.98) | 2.50 (1.38) ^a |
| CA1 subfield | 1.26 (0.47) | 1.48 (0.49) | 1.99 (0.82) ^b |
| CA3 subfield | 1.86 (1.18) | 1.69 (0.82) | 1.93 (1.48) |
| Dentate gyrus | 1.51 (1.02) | 0.78 (0.88) | 1.47 (1.00) |
| Posterior hippocampus | 1.98 (0.52) | 2.08 (0.51) | 1.88 (1.10) |
| Prefrontal cortex | | | |
| Gyrus rectus | 2.13 (0.96) | 2.08 (0.60) | 1.92 (0.96) |
| Medial orbitofrontal cortex | 1.36 (1.06) | 2.03 (0.84) | 2.51 (1.00) ^b |
| Dorsolateral prefrontal cortex | 2.35 (0.56) | 2.09 (0.60) | 1.79 (0.84) ^c |
| Ventral striatum | | | |
| Caudate | 1.78 (0.43) | 1.70 (0.63) | 2.05 (1.16) |
| Nucleus accumbens | 1.88 (0.52) | 2.16 (0.71) | 2.04 (1.16) |
| Putamen | 2.32 (0.52) | 1.98 (0.64) | 2.07 (0.84) |
| Amygdala | | | |
| Dorsal nucleus | 1.30 (1.02) | 1.41 (1.61) | 1.22 (1.59) |
| Basolateral nucleus | 1.04 (1.03) | 1.49 (0.55) | 1.50 (1.03) |

^a $P < .10$ for controls vs patients with schizophrenia by analysis of variance.

^b $P < .01$ for controls vs patients with schizophrenia by analysis of variance.

^c $P < .05$ for controls vs patients with schizophrenia by analysis of variance.